

# Perfect imaging: they don't do it with mirrors

Ulf Leonhardt and Sahar Sahebdivan

School of Physics and Astronomy, University of St Andrews,  
North Haugh, St Andrews KY16 9SS, UK

January 26, 2023

## Abstract

Imaging with a spherical mirror in empty space is compared with the case when the mirror is filled with the medium of Maxwell's fish eye. Exact time-dependent solutions of Maxwell's equations show that perfect imaging is not achievable with an electrical ideal mirror on its own, but with Maxwell's fish eye in the regime when it implements a curved geometry for full electromagnetic waves.

# 1 Introduction

Perfect imaging with positive refraction [1, 2, 3, 4, 5] challenges [6, 7, 8, 9] some of the accepted wisdom [10] of subwavelength imaging: it does not appear to perform an amplification of evanescent waves [10] and requires a drain at the image in the stationary regime [3]. Yet it seems to work, at least, for the time being, in theory. To illuminate some of the perceived paradoxes of perfect imaging, it is instructive to consider the simplest possible case [9]: imaging with a spherical mirror. In this paper, the imaging with such a mirror is compared with the imaging in Maxwell’s fish eye [4]. Exact time-dependent solutions of Maxwell’s equations reveal the similarities and characteristic differences between the two cases; the mirror cannot perfectly image, but Maxwell’s fish eye can.

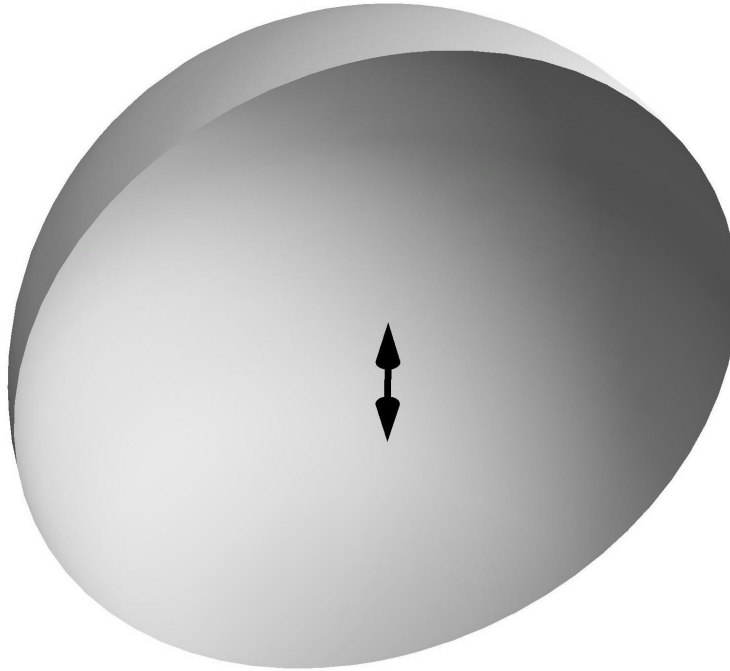


Figure 1: Spherical mirror. In this paper we consider the electromagnetic wave emitted by a point dipole (double arrow) in the centre of a perfect spherical mirror (half sphere — only half of the mirror is shown for being able to see the interior). We compare this case with imaging in Maxwell’s fish eye in three dimensions [4].

Imagine a point dipole placed at the centre of a spherically symmetric mirror that completely surrounds it (Fig. 1). The dipole emits electromagnetic radiation that reaches the mirror, is reflected there, travels back and focuses at the centre where the dipole sits — the dipole is imaged to itself. Due to the symmetry of the sphere, this is the simplest conceivable imaging problem. Within the regime of geometrical optics [11], the focusing with the mirror would be perfect, but the highly concentrated field in the centre violates the validity condition of geometrical optics [11]. Therefore, exact calculations of the complete Maxwell equations are

required for elucidating the imaging performance of the mirror. The same applies to Maxwell's fish eye [1, 2, 3, 4] where we fill the space enclosed by the mirror with a dielectric material that has a certain radially symmetric graded refractive index  $n(r)$ . To simplify the algebra, we shall measure space in units of the mirror radius; in these units the mirror surrounds the dipole at radius

$$r = 1 \quad (\text{mirror}). \quad (1)$$

It is also advantageous to measure the time  $t$  in units of the distance traveled in free space; in these units we obtain for the speed of light in vacuum

$$c = 1. \quad (2)$$

We consider the propagation of electromagnetic waves in three-dimensional space, a case where the theory is mathematically simpler than in two-dimensional wave propagation. In 3D, however, impedance matching is required for perfect imaging where the electric permittivity  $\varepsilon$  equals the magnetic permeability  $\mu$ , which is difficult to achieve for materials in practice (but trivially the case in empty space). For the sake of theoretical simplicity we require

$$\varepsilon = \mu = n(r). \quad (3)$$

In empty sphere, the refractive index is unity:

$$n = 1 \quad (\text{empty space}) \quad (4)$$

and in the case when we fill the sphere with Maxwell's fish eye we have [1]

$$n = \frac{2}{1 + r^2} \quad (\text{Maxwell's fish eye}). \quad (5)$$

Equations (1)-(5), together with Maxwell's equations of electromagnetism, set the scene for the problem we investigate in this paper: the radiation of a dipole placed at  $r = 0$ . But before we address this problem a few (well-known) ideas on causality are needed.

## 2 Causality

Maxwell's electromagnetism is completely time-reversible; a dipole may emit an electromagnetic wave, but it may as well absorb the same wave run in reverse — by carefully choosing the initial conditions at the boundary an electromagnetic wave may focus at the dipole and be completely absorbed. The latter solutions of Maxwell's equations, where the interaction of the wave with the dipole lies in the future, are called *advanced*, whereas the former solutions, where the dipole causes the emission of the wave, are called *retarded* (Fig. 2). Clearly, in our case retarded solutions are required; they are causal: no radiation is present prior to the event of emission at, say, time  $t = 0$ . We thus require for all field quantities  $G$ :

$$G(t) = 0 \quad \text{for} \quad t < 0. \quad (6)$$

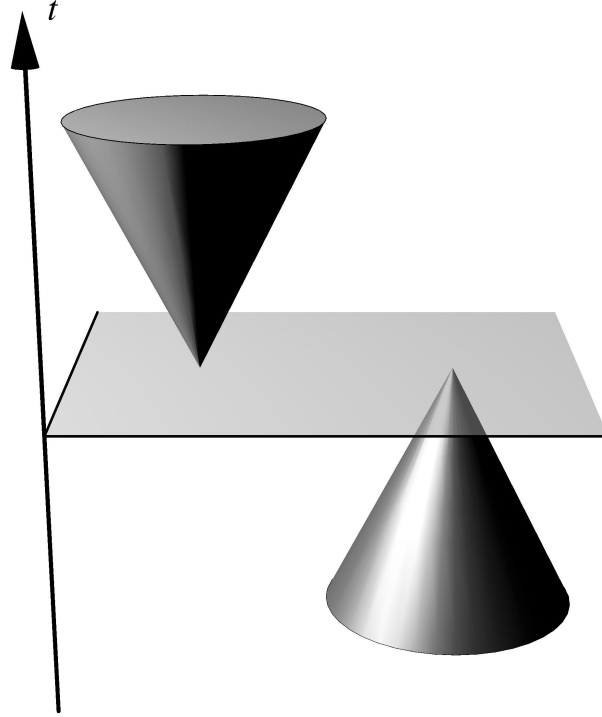


Figure 2: Schematic space–time diagram of retarded waves (left) and advanced waves (right). The retarded wave is causal; it is created at some moment in time indicated by the planar sheet in the space–time diagram. Prior to that time the wave amplitude is strictly zero. On the other hand, the advanced wave converges into a single spatial point and vanishes there; it is zero after a certain time. Maxwell’s equations have both retarded and advanced solutions and superpositions of the two, but only the retarded waves are causal.

Suppose we represent the quantity  $G$  in terms of its Fourier components  $\tilde{G}$ :

$$G(t) = \int_{-\infty}^{+\infty} \tilde{G}(\omega) e^{-i\omega t} d\omega. \quad (7)$$

The causality condition (6) is met if  $\tilde{G}(\omega)$  is analytic on the upper half complex  $\omega$  plane and decays sufficiently fast, such that we can close the integration contour of the Fourier integral (7) on the upper half plane for  $t < 0$  when  $\exp(-i\omega t)$  decays for  $\text{Im } \omega > 0$ ; if  $\tilde{G}(\omega)$  is analytic the closed-contour integral is zero and  $G$  vanishes for  $t < 0$ , as required (Fig. 3). Conversely, in the causal case (6) we obtain from the inverse Fourier transformation

$$\tilde{G}(\omega) = \frac{1}{2\pi} \int_0^{+\infty} G(t) e^{i\omega t} dt \quad (8)$$

that  $\tilde{G}(\omega)$  obeys the defining Cauchy–Riemann differential equations of analytic functions, because the only frequency–dependent term  $\exp(i\omega t)$  in the integral (8)

is analytic, provided the integral (8) converges. Convergence is guaranteed, because  $\text{Re}(i\omega t) < 0$  for  $\text{Im}\omega > 0$  and  $t > 0$  and so the integrand exponentially decays. Furthermore, in the limit  $\text{Im}\omega \rightarrow \infty$  the term  $\exp(i\omega t)$  tends to zero, so  $\tilde{G}$  decays at  $\infty$  on the upper half plane. We conclude that the Fourier transform of causal fields must be analytic and decaying on the upper half plane. We use this requirement to deduce the causal solutions for our imaging problem.

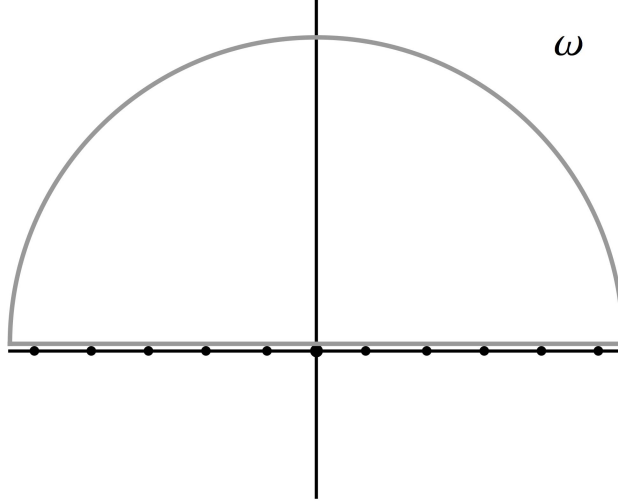


Figure 3: Causality on the complex frequency plane. The Fourier transform of causal waves (Fig. 2) must be analytic and decaying on the upper half complex  $\omega$  plane. The singularities (dots) of the Fourier transform lie on the lower half plane or, as in this picture, on the real axis. In such a case, the contour (grey line) of the Fourier integral (7) can be closed on the upper half plane for  $t < 0$  and the integration gives zero, as required by causality (6). The picture shows the first 11 singularities (23) of the Fourier-transformed vector potential of dipole radiation in the spherical mirror (Fig. 1).

### 3 Symmetry

Consider a radially-symmetric impedance-matched medium (3) inside the spherical mirror at radius (1) and suppose that a point dipole is placed at the centre that emits a flash of light. To describe the electromagnetic wave emitted by the dipole we use spherical polar coordinates  $\{r, \theta, \phi\}$  with  $z$  axis aligned to the dipole. We assume that the vector potential  $\mathbf{A}$  of the wave points in the direction of the dipole with an amplitude  $A$  that only depends on the radius  $r$  (our calculations will show that this assumption is consistent with Maxwell's equations). We thus require

$$A_i = A(r, t) (\cos \theta, -r \sin \theta, 0) \quad (9)$$

in spherical polars where  $(\cos \theta, -r \sin \theta, 0)$  is the unit one-form in  $z$  direction [12]. We obtain the magnetic field  $\mathbf{B}$  from  $\mathbf{B} = \nabla \times \mathbf{A}$  where for our ansatz (9) in

spherical polars [12]

$$B_r = 0, \quad B_\theta = 0, \quad B_\phi = B \sin^2 \theta \quad (10)$$

with the magnetic-field amplitude in the plane of emission (for  $\theta = \pi/2$ )

$$B = -r \partial_r A. \quad (11)$$

We use the symbol  $\partial_r$  to abbreviate the partial derivative  $\partial/\partial r$  and we are going to use  $\partial_t$  for  $\partial/\partial t$ . From Maxwell's equation  $\partial_t \varepsilon \mathbf{E} = \nabla \times \mu^{-1} \mathbf{B}$  with our units (2) and in the medium (3) follows

$$\partial_t E_r = \frac{2B}{n^2 r^2} \cos \theta, \quad \partial_t E_\theta = -\frac{1}{n} \partial_r \frac{B}{n} \sin \theta, \quad \partial_t E_\phi = 0. \quad (12)$$

Furthermore, from Faraday's law  $\nabla \times \mathbf{E} = -\partial_t \mathbf{B}$  we obtain the wave equation

$$\partial_r \frac{1}{n} \partial_r \frac{B}{n} - \frac{2B}{n^2 r^2} = \partial_t^2 B. \quad (13)$$

All other components of  $\nabla \times \partial_t \mathbf{E}$  vanish for the electric field (12) in spherical polars, which reduces the problem to the wave equation (13) and justifies our ansatz (9). Finally, we require that the mirror acts as an ideal electrical mirror where the electric-field components in the mirror are put to zero, in our case (1)

$$E_\theta|_{r=1} = 0, \quad (14)$$

which implies from expression (12) that

$$\partial_r B|_{r=1} = 0. \quad (15)$$

We see that the magnetic field must not change at the mirror. In the following we seek causal solutions of the wave equation (13) with boundary condition (15) for the magnetic field  $B$  expressed in terms (11) of the vector potential. First we consider the dipole radiation in empty space surrounded by the spherical mirror [9] and then we compare this case with Maxwell's fish eye [4].

## 4 Mirror

In empty space (4) the left-hand side of the wave equation (13) for the magnetic field (11) reduces to

$$\partial_r^2 B - \frac{2B}{r^2} = -r \partial_r \left( \partial_r^2 A + \frac{2}{r} \partial_r A \right) \quad (16)$$

such that the wave equation (13) is satisfied if

$$\partial_r^2 A + \frac{2}{r} \partial_r A = \partial_t^2 A. \quad (17)$$

The vector potential thus obeys the usual radial wave equation with the general solution

$$\tilde{A} = \frac{\mathcal{A}_+}{r} e^{i\omega r} + \frac{\mathcal{A}_-}{r} e^{-i\omega r} \quad (18)$$

for waves with Fourier components  $\tilde{A}$ . Note that in our units (2) the frequency  $\omega$  is equal to the wave number that normally appears in the spherical waves (18). The first term of expression (18) describes an outgoing wave and the second term an ingoing wave. The spherical mirror turns outgoing into ingoing waves and so we expect that the coefficients  $\mathcal{A}_\pm$  are not independent. Indeed, we obtain from condition (15) for the magnetic field (11) of the wave (18)

$$\mathcal{A}_- = -\mathcal{A}_+ e^{2i\omega} \frac{\omega^2 + i\omega - 1}{\omega^2 - i\omega - 1} = -\mathcal{A}_+ e^{2i\omega + 2i\delta} \quad (19)$$

where  $\delta$  denotes the phase

$$\delta = \arctan\left(\frac{\omega}{\omega^2 - 1}\right). \quad (20)$$

At the mirror (1) the outgoing component  $\mathcal{A}_+ \exp(i\omega r)$  thus produces the ingoing component  $\mathcal{A}_- \exp(-i\omega r)$  and vice versa, apart from the extra phase (20). This phase vanishes for high frequencies  $\omega \rightarrow \infty$  where the wavelength approaches zero and imaging becomes perfect, regardless whether it is subwavelength-limited or not. For finite  $\omega$  the phase (20) is responsible for limiting the resolution of the mirror, as we see next.

Let us write down the following combination of outgoing and ingoing waves (18)

$$\tilde{A} = \frac{\sin(\omega - \omega r + \delta)}{r \sin(\omega + \delta)}. \quad (21)$$

One verifies that this  $\tilde{A}$  obeys the condition (19) of spherical waves reflected by the mirror. We also see that

$$\tilde{A} \sim r^{-1} \quad \text{for } r \rightarrow 0, \quad (22)$$

which shows that the electromagnetic wave is generated by a point dipole at the centre (the wave equation (17) produces a source term that is proportional to a spatial delta function). The Fourier components (21) thus constitute the electromagnetic field of a light flash emitted by a point dipole, if they are causal, i.e. analytic and decaying on the upper half  $\omega$  plane. Representing the sine functions in expression (21) in terms of exponentials we see that  $\tilde{A} \rightarrow 0$  for  $\omega \rightarrow \infty$ . Furthermore,  $\tilde{A}$  is analytic, apart from poles  $\omega_m$  on the real axis (Fig. 3) where

$$\sin(\omega_m + \delta_m) = 0. \quad (23)$$

The Fourier transform  $\tilde{A}$  also has a quadratic singularity at  $\omega = 0$ . In order to obtain a causal solution we must move the poles slightly below the real axis, by providing  $\omega$  with an infinitesimal, positive imaginary part. Alternatively, we move the integration contour up from the real axis by an infinitesimal distance (Fig. 3).

In both cases, we can close the contour of the Fourier integral (7) on the upper half plane for  $t < 0$  and get zero, as required for causal waves (6). For  $t > 0$  we close the contour on the lower half plane and obtain from Cauchy's theorem

$$A = \frac{2}{\pi r} \sum_{m=1}^{\infty} \eta_m \sin(\omega_m r) \sin(\omega_m t) \quad (24)$$

with the coefficients

$$\eta_m = \frac{\omega_m^4 - \omega_m^2 + 1}{\omega_m^4 - 2\omega_m^2}. \quad (25)$$

For the light flash emitted by the dipole in the centre of the mirror, we obtained the exact solution (24) with the pole frequencies (23) and the coefficients (25). Let us investigate the extent to which this wave images the dipole onto itself.

For perfect imaging we require that an outgoing wave is perfectly converted into an ingoing wave. The wave is focused at the centre and bounces back and forth with a period of twice the time it takes to travel to the mirror, 2 in our units. As a flash of light is described by a radial delta function, the flash in a perfectly imaging device should be given in terms of the periodic delta function  $\Delta(t)$  of period 2, i.e. the kernel of the discrete Fourier transform

$$\Delta(t) = \frac{1}{2\pi} \sum_{m=1}^{\infty} e^{im\pi t} = \frac{1}{2\pi} + \frac{1}{\pi} \sum_{m=1}^{\infty} \cos(m\pi t). \quad (26)$$

At the mirror (1), the wave changes sign and propagates backwards. We thus require for the radial wave  $A_0$  in the case of perfect imaging of the dipole onto itself

$$A_0 = \frac{\Delta(t-r)}{r} - \frac{\Delta(t+r-2)}{r}. \quad (27)$$

Writing  $A_0$  in terms of the periodic delta function  $\Delta$  guarantees that  $A_0$  is periodic with period 2. We obtain from expression (26)

$$A_0 = \frac{2}{\pi r} \sum_{m=1}^{\infty} \sin(m\pi r) \sin(m\pi t). \quad (28)$$

Formula (28) strongly resembles our result (24) for the spherical mirror, but not perfectly. There, instead of the eigenfrequencies  $m\pi$  the pole frequencies  $\omega_m$  appear and the trigonometric series (24) contains the coefficients  $\eta_m$ . The poles (23) depend on the phase (20) that, for large  $\omega$ , approaches  $\omega^{-1}$ . In this limit we obtain for the poles (23)

$$\omega_m = \pm \left( \frac{m\pi}{2} + \sqrt{\frac{m^2\pi^2}{4} - 1} \right) \quad (\text{integer } m) \quad (29)$$

that approaches  $m\pi$  for  $m \rightarrow \infty$ . In this limit also  $\eta_m \rightarrow 1$ , as we see from expression (25). Consequently, whenever large- $m$  components dominate the series (28) of the perfect wave, they also dominate the wave (24) in the spherical mirror. We see from definition (27) that this is the case at the infinitely peaked front of the light flash



bouncing back and forth in the mirror. Therefore, the perfectly imaging wave makes the dominant contribution to the electromagnetic wave in the spherical mirror.

Figure 4 shows the difference  $A - A_0$  between the vector potential (24) of the light reflected in the spherical mirror and perfectly reflected light flashes (27). Relativistic causality implies that the outgoing wave  $A$  must remain a perfect pulse until it hits the mirror. Therefore the deviation from the ideal vector potential  $A_0$  cannot correspond to any physical field. Figure (4) indicates that, during this stage,  $A - A_0$  is constant in space but grows in time. This growth must be linear in order for  $A$  to obey the radial wave equation (17). As the magnetic field (11) and the electric field (12) depend on the spatial derivative of  $A$  in the gauge relevant to our ansatz (9), the electromagnetic fields do not deviate from free dipole radiation until the wave hits the mirror. After the first reflection the wave is no longer a perfect pulse: the vector potential carries an additional discontinuity at the position of the pulse and develops a field in its wake. Note that the mirror is not assumed to be dispersive or otherwise imperfect; these features quantify the imperfections of imaging with an ideal spherical mirror.

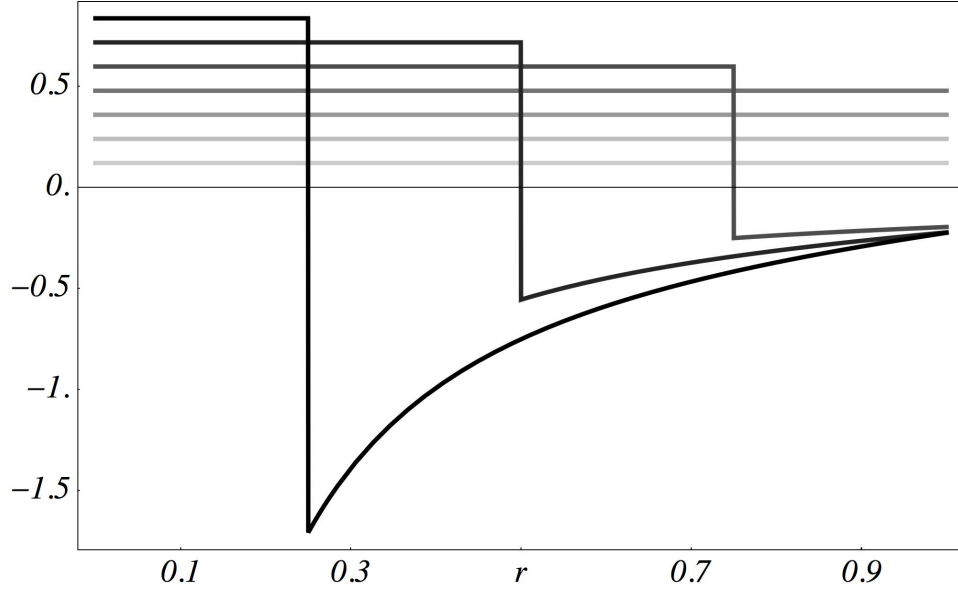


Figure 4: The reflection of a light pulse in an ideal electrical mirror is not perfect. The figure shows the difference  $A - A_0$  between the amplitude (24) of the vector potential  $A(r)$  of dipole radiation in the spherical mirror and the amplitude (27) of a perfectly reflected infinitely peaked pulse  $A_0(r)$ . The different shades of grey indicate the different evolution times  $t = 0.25, 0.5, 0.75, 1.0, 1.25, 1.5, 1.75$  in our units, the lighter the tone the earlier is the time. One sees that before the pulse has reached the mirror at  $r = 1$  the amplitude of the radial vector potential is uniform in space but grows linearly in time. After the interaction with the mirror the amplitude develops an additional discontinuity at the position of the pulse and a field in its wake (see also Fig. 5).

## 5 Perfection

Now imagine we fill the space enclosed by the mirror with the impedance-matched (3) medium (5) of Maxwell's fish eye [1]. This device implements the geometry of a curved space. In particular, it creates the illusion that light propagates on the 3-dimensional surface of the 4-dimensional hypersphere [2]. It turns out [4] that the geometry of waves in Maxwell's fish eye appears in the clearest possible form if we write the vector potential  $A$  as

$$A = 2 \int (\partial_r D) n dr \quad \text{or, equivalently,} \quad \partial_r A = 2n \partial_r D \quad (30)$$

or, from definition (11),

$$B = -2nr \partial_r D. \quad (31)$$

We show next that the function  $D$  is the scalar Green function on the hypersphere [4]. For this we inspect the left-hand side of the wave equation (13) where

$$\partial_r \frac{1}{n} \partial_r \frac{B}{n} - \frac{2B}{n^2 r^2} = -2nr \partial_r \left( \frac{1}{n^3 r^2} \partial_r n r^2 \partial_r D - D \right). \quad (32)$$

Therefore the wave equation is satisfied if  $D$  obeys

$$\frac{1}{n^3 r^2} \partial_r n r^2 \partial_r D - D = \partial_t^2 D. \quad (33)$$

This is the conformally-coupled radial scalar wave equation on the virtual space implemented by Maxwell's fish eye, the surface of the hypersphere [4]. Consequently, if  $D$  satisfies the boundary condition (15) at the mirror and contains a point source at the centre,  $D$  is the scalar Green function on the hypersphere. Let us construct this Green function. One easily verifies the following expression for the two fundamental solutions of the Fourier-transformed wave equation (33):

$$\tilde{D}_\pm = \frac{1}{2} \left( r + \frac{1}{r} \right) \exp(\pm 2i\omega \arctan r). \quad (34)$$

In order to implement the boundary condition (15) imposed by the mirror we exploit the fact [4] that the wave equation (33) is invariant under the transformation  $r \rightarrow r^{-1}$ . In particular, it is elementary to see from the explicit solutions (34) and the relation  $\arctan r^{-1} = \pi - \arctan r$  that

$$\tilde{D}_\pm(r^{-1}) = e^{\pm 2i\pi\omega} \tilde{D}_\mp(r). \quad (35)$$

Let us put

$$\tilde{D} = \tilde{D}_+(r) + \tilde{D}_+(r^{-1}). \quad (36)$$

Relation (35) proves that this linear combination obeys the wave equation (33). One verifies that it also satisfies the boundary condition (15) at the mirror. Furthermore, from expressions (34) and (35) follows that the combination (36) is analytic and exponentially decaying on the upper half complex  $\omega$  plane for  $0 < r < 1$ , i.e. within

the space enclosed by the mirror. Consequently, the Fourier-transformed amplitude (36) describes a causal wave.

To see whether the solution (36) corresponds to the electromagnetic wave generated by the point dipole at the centre, we need to investigate its behavior when  $r \rightarrow 0$ . We obtain from expressions (34)-(36) that

$$\tilde{D} \sim \frac{1}{2r} (1 + e^{i\pi\omega}) \quad \text{for } r \rightarrow 0. \quad (37)$$

The function  $D$  thus develops the characteristic  $r^{-1}$  singularity of a point source — it thus corresponds to the field emitted by a point dipole, whereas the prefactor  $1/2$  accounts for the value of 2 of the refractive index (5) at the point of emission at  $r = 0$ . This proves that the solution (36) describes dipole radiation. But we also see that the electromagnetic wave attains the phase factor  $\exp(i\pi\omega)$ . This factor must come from the reflected wave. Reflection at the mirror results in a sign flip of the field, but the factor  $\exp(i\pi\omega)$  carries a plus sign, which means that the dipole at the centre acts as a drain for the reflected wave. In order to maintain a stationary regime in perfect imaging, an additional drain is required at the image [3], in our case, the centre.

Why is this not the case in imperfect imaging? Suppose that for our previous example, empty space enclosed by the spherical mirror, we follow the same procedure and form the following linear combination of the two fundamental solutions (18) with the reflection condition (19):

$$\tilde{A} = \frac{1}{r} (e^{i\omega r} - e^{2i\omega + 2i\delta - i\omega r}) , \quad e^{2i\delta} = \frac{\omega^2 + i\omega - 1}{\omega^2 - i\omega - 1}. \quad (38)$$

This expression develops poles at the zeros of  $\omega^2 - i\omega - 1$ , i.e. at

$$\omega = \frac{i \pm \sqrt{3}}{2}, \quad (39)$$

on the upper half plane! Therefore, the solution (38) is not causal, the drain is not causally connected to the source, but rather acts as an independent source of radiation. However, as we have seen, Maxwell's fish eye makes all the difference here; in this case the drain is an inevitable consequence of causality for maintaining a stationary flow of radiation.

The introduction of a drain for perfect imaging in the stationary regime may still be perceived as a paradox, but it is no longer relevant in time-dependent solutions of Maxwell's equations. In the case of the empty mirror we found the clearest description of the physics involved in imaging by discussing time-dependent pulses, and we expect the same in the case of Maxwell's fish eye. There we obtain from the Fourier integral (7) and expressions (34)-(36)

$$\begin{aligned} D &= \int_{-\infty}^{+\infty} \tilde{D}(\omega) e^{-i\omega t} d\omega \\ &= \pi (r + r^{-1}) [\delta(2 \arctan r - t) + \delta(2 \arctan r^{-1} - t)] \\ &= 2\pi \delta(\cos t + \zeta) + 2\pi \delta(\cos t - \zeta), \quad \zeta = \frac{r^2 - 1}{r^2 + 1} \end{aligned} \quad (40)$$

where the  $\delta$  denote delta functions. From relation (30) follows that the vector potential  $A$  consists of corresponding delta functions as well. We see clearly from formula (40) that the field is bouncing back and forth between the centre of the sphere and the mirror without changing its shape: the imaging is perfect (Fig. 5).

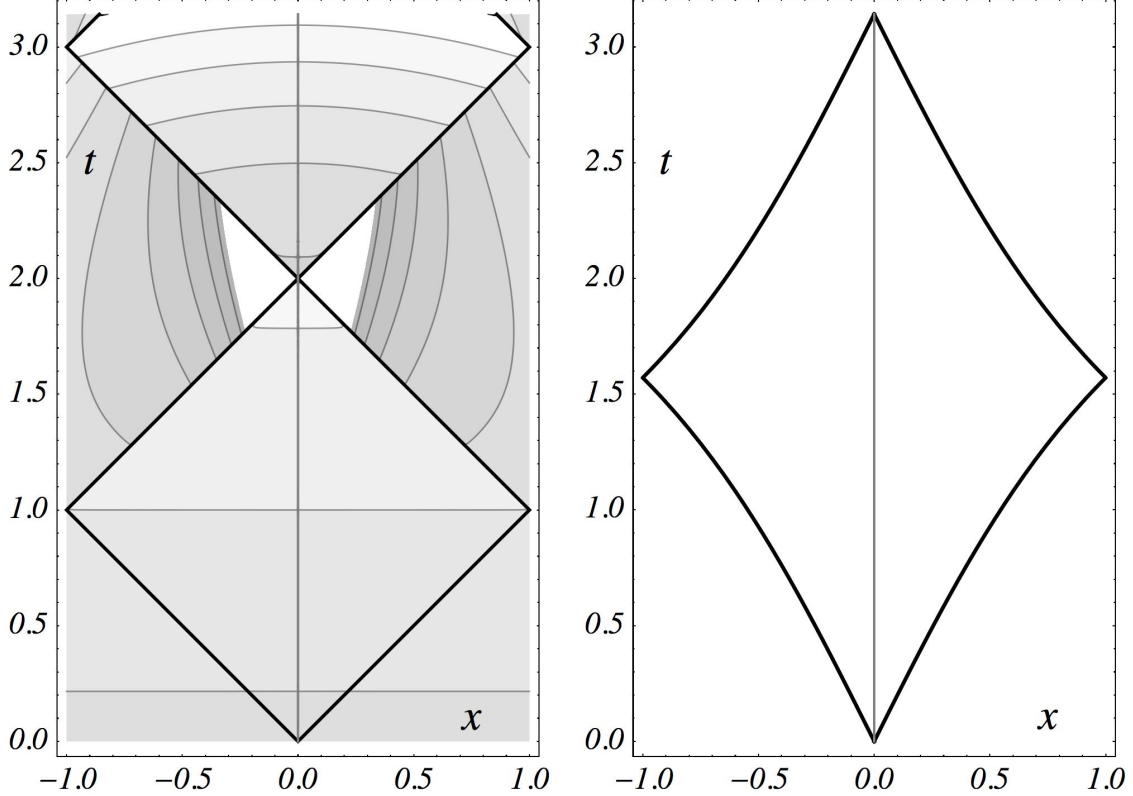


Figure 5: Mirror versus Maxwell's fish eye. Space-time diagrams of the vector potential of light flashes evolving in time (left) for imaging in a spherical mirror and (right) in Maxwell's fish eye supplemented by a mirror. The mirror is placed at the vertical boundaries of each diagram where the grey vertical line indicates the world line of the centre. The black curves correspond to the infinite peaks of the flashes, the contours describe the finite values of the vector potential. As the right picture contains no finite contours, just infinite peaks, the flash is not disintegrating and bounces back and forth between the mirror in Maxwell's fish eye: imaging is perfect there. In contrast, the left picture shows the imperfections arising from reflection in an ideal electrical mirror: after the flash has bounced off the mirror the vector potential carries an additional discontinuity and a field in its wake that develops a singularity at the refocusing time  $t = 2$  in our units (the contours are cut off around the singularity). After that time the entire interior of the mirror is filled with a spatially non-uniform vector potential that corresponds to a non-vanishing electromagnetic field distorting the flash: perfect imaging is not done with mirrors.

## 6 Credo

An ideal spherical mirror cannot perfectly image on its own, the mirror inevitably distorts light pulses (left of Fig. 5). However, if the space enclosed by the mirror is filled with the medium of the impedance-matched Maxwell fish eye, pulses are no longer distorted and thus the imaging is perfect (right of Fig. 5). We have seen that the introduction of a drain at the image is a consequence of causality in the stationary regime, but is not required for light pulses. On the other hand, in imperfect imaging the drain would be in conflict with causality. One of the puzzles of perfect imaging with positive refraction seems to be resolved.

Yet one may still wonder how Maxwell’s fish eye is able to restore evanescent waves in a similar way negative refraction does [10]. But note that the amplification of evanescent waves is not the only physical picture explaining the performance of the negatively-refracting perfect lens; there is a simple geometrical argument [13]: the lens performs a folding transformation of space [14]. The negative-index lens appears to fold the space perceived by electromagnetic waves such that three regions are identical, one region in front of the device, the lens itself, and the region behind it (Fig. 6). As these regions are identical for the field, the field strength of an electromagnetic waves must be exactly the same at all triples of connected points: negative refraction makes a perfect lens by spatial transformation [13]. In this geometrical picture of imaging we do not need to discriminate between evanescent and propagating waves, because the electromagnetic field is transformed in its entirety.

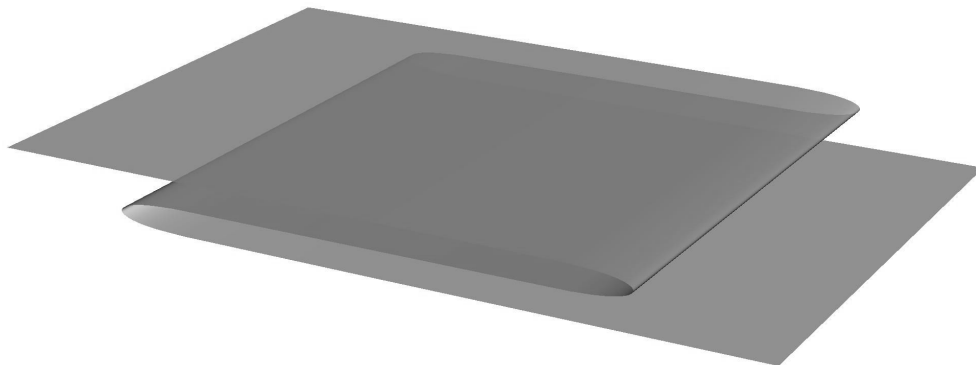


Figure 6: Negative refraction and folding of space. The figure illustrates the geometrical representation [13] of perfect imaging by negative refraction: the device appears to fold space such that the entire electromagnetic field in the folded regions is identical — the device transfers the field from one region into another: imaging is perfect. Note that this geometrical picture does not discriminate between propagating and evanescent waves.

Geometry also explains the perfect imaging with Maxwell’s fish eye that has a positive refractive-index profile. Like in the case of the perfect lens, this device changes the geometry of space for the electromagnetic field. It creates the effect that electromagnetic waves propagate in the 3-dimensional surface of the 4-dimensional hypersphere. Imagine an ordinary 3-dimensional sphere with 2-dimensional curved surface (the hypersphere is not much different). Suppose light is confined to the

surface. There it is completely natural that light waves emitted at any point of the sphere converge on its antipodal point (left of Fig. 7). In Maxwell’s fish eye, the antipodal point on the virtual sphere corresponds to the image point in physical space. In the case discussed in this paper, we cut the fish eye by a spherical mirror that, in virtual space, appears as a mirror around the equator of the sphere (right of Fig. 7). The introduction of the mirror is not essential for perfect imaging in theory, but it is vital in practice, for limiting the index range and avoiding superluminal propagation [3]. The mirror creates the illusion that light explores the entire sphere, whereas in reality it is confined to the semi-sphere where the index range in physical space is smallest. Such conjuring tricks with mirrors are only possible in curved space. Moreover, the imaging of Maxwell’s fish-eye, with or without mirror, is not restricted to a single point but happens for all points. This is possible for devices that implement perfect, curved geometries beyond the approximation of geometrical optics. In such cases, the virtual geometry of light created by the material is valid for full electromagnetic waves. Perfect imaging is not done with mirrors [15], but with geometry.

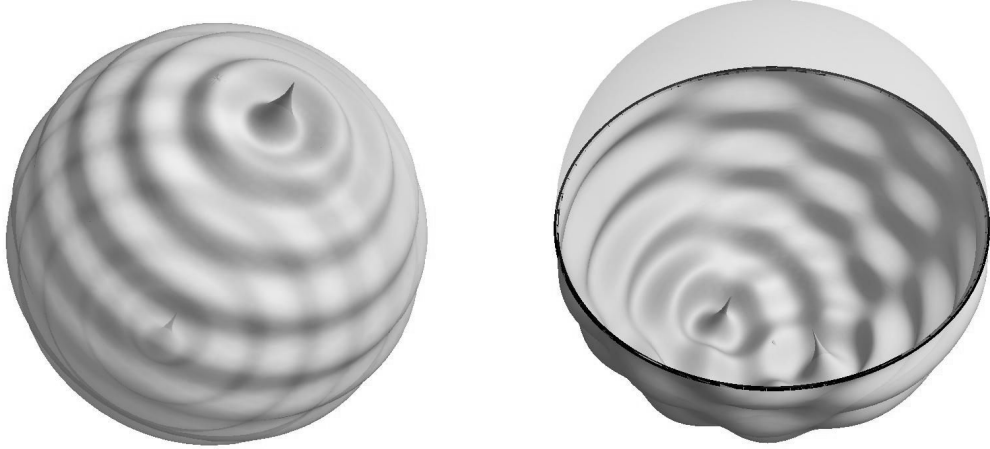


Figure 7: Geometry behind Maxwell’s fish eye. Luneburg [2] discovered that Maxwell’s fish eye implements in 2D the geometry of the two-dimensional surface of a 3D sphere (or in 3D the three-dimensional surface of the 4D hypersphere). The figure illustrates the 2D case [3]. The left picture shows a wave on the sphere emitted from a point source and forming a perfect image at its antipodal point. In the right picture a circular mirror is placed at the equator of the sphere such that the image remains on the southern hemisphere [3] that corresponds to a finite region in physical space. In 3D a spherical mirror should be used. Source and image merge when the source is placed at the south pole, which in physical space corresponds to emission from the centre of Maxwell’s fish eye, the case considered in this paper.

## Acknowledgements

We thank Merlin for discussions and the Royal Society for support.

## References

- [1] J.C. Maxwell, Cambridge and Dublin Math. J. **8**, 188 (1854).
- [2] R.K. Luneburg, *Mathematical Theory of Optics* (University of California Press, Berkeley and Los Angeles, 1964).
- [3] U. Leonhardt, New J. Phys. **11**, 093040 (2009).
- [4] U. Leonhardt and T.G. Philbin, Phys. Rev. A **81**, 011804 (2010).
- [5] P. Benitez, J.C. Miñano, and J.C. González, Opt. Express **18**, 7650 (2010).
- [6] R.J. Blaikie, New J. Phys. **12**, 058001 (2010).
- [7] U. Leonhardt, New J. Phys. **12**, 058002 (2010).
- [8] S. Guenneau, A. Diatta, and R.C. McPhedran, J. Mod. Optics **57**, 511 (2010).
- [9] R. Merlin, arXiv:1007.0280.
- [10] J.B. Pendry, Phys. Rev. Lett. **85** 3966 (2000).
- [11] M. Born and E. Wolf, *Principles of Optics* (Cambridge University Press, Cambridge, 1999).
- [12] U. Leonhardt and T.G. Philbin, Prog. Opt. **53**, 69 (2009).
- [13] U. Leonhardt and T.G. Philbin, New J. Phys. **9**, 254 (2007).
- [14] H. Chen, C.T. Chan, and P. Sheng, Nature Materials **9**, 387 (2010).
- [15] A. Christie, *They Do It With Mirrors*, (Penguin, Harmondsworth, 2000).